are the numerical results. For the TM waves, the difference between the results produced by H and E formulations is very small, thereby the two methods are practically equivalent. As an example for the three-dimensional structures, we calculated the field patterns of the fundamental H_{11}^{y} mode of a square channel waveguide. The refractive indices of the core and the cladding are $n_1 = 1.5$ and $n_2 = 1.3$, respectively. The width and the height of the core is $w = h = 1$ μm. The wavelength is $\lambda = 1.5$ μm. The window sizes are 3×3 μm and the total number of points are 51×51. The dominant H_y and the associated H_x components are shown in Fig. 3(a) and (b). The hybrid nature of the mode in the channel waveguide is clearly illustrated. In comparison with the field patterns for the transverse electric fields [9], the transverse magnetic fields are seen to be continuous all over the cross section.

In conclusion, a formulation based on the transverse electric fields for the vector beam propagation method is proposed and presented. It is shown that the FD-VBPM based on the H formulation is equivalent to that based on the E formulation. The FD-VBPM based on the magnetic fields may be used for the modeling and simulation of the vectorial wave propagation in a wide range of practical optical guided-wave structures.

References

[1] M. D. Feit and J. A. Fleck, Jr. "Light propagation in graded-index optical fibers," *Appl. Opt.*, vol. 17, no. 24, pp. 3990-3998, 1978.

[2] D. Yevick and B. Hermansson, "Efficient beam propagation techniques," *IEEE J. Quantum Electron.*, vol. 26, no. 1, pp. 109-112, 1990.

[3] T. B. Koch, J. B. Davies, and D. Wickramasinghe, "Finite element/finite-difference propagation algorithm for integrated optical devices," *Electron. Lett.*, vol. 25, no. 8, pp. 514-516, 1989.

[4] Y. Chung and N. Dagli, "An assessment of finite-difference beam propagation method," *IEEE J. Quantum Electron.*, vol. 26, no. 8, pp. 1335-1339, 1990.

[5] J. Gerdes and P. Pregla, "New beam-propagation algorithm based on the method of lines," *J. Opt. Soc. Amer. B.*, vol. 8, no. 2, pp., 1991.

[6] R. Clauberg and P. Von Allmen, "Vectorial beam-propagation method for integrated optics," *Electron Lett.*, vol. 27, no. 8, pp. 654-655, 1991.

[7] W. P. Huang, C. L. Xu, S. T. Chu, and S. K. Chaudhuri, "A vector beam propagation method for guided-wave optics," *IEEE Photon. Technol. Lett.*, to be published.

[8] —, "The finite-difference vector beam propagation method. Analysis and assessment," *J. Lightwave Technol.*, to be published.

[9] W. P. Huang, C. L. Xu, and S. K. Chaudhuri, "The finite-difference vector beam propagation method for three-dimensional waveguide structures," *IEEE Photon. Technol. Lett.*, to be published.

Propagation Characteristics of GaAs/AlGaAs QW Ridge Waveguides

V. R. Chinni, C. R. Menyuk, and Y. J. Chen

Abstract—**A method is presented which allows us to accurately determine geometric effects in QW devices. Finite element methods have been used in combination with perturbation techniques to determine the propagation characteristics of a single QW GaAs/AlGaAs ridge waveguide. The attenuation coefficient and phase shift are evaluated for both TE and TM polarizations. The results show that a simple slab model overestimates the attenuation and phase change for wavelengths smaller than the excitonic resonances of the QW and underestimates them for larger wavelengths.**

Introduction

THERE is a growing interest in quantum well waveguides and other associated optoelectronic devices such as lasers, modulators, and switches. Lateral confinement of the mode is produced in such devices by etching the top layer and thereby producing a ridge structure. The ridge also determines the propagation constant and mode field distribution across the guide. The effects of a QW in waveguides with simple geometries can be calculated with a simple model [1] but waveguides with more complex geometries require more detailed calculations. The electric field experienced by the QW layer due to voltage applied across the waveguide will be nonuniform because of the presence of the ridge. Therefore, the guided wave experiences different perturbations at different lateral positions of the QW, and the total absorption and phase change depend upon the waveguide geometry.

In this letter a method is presented which includes the geometry of the waveguide to determine excitonic contributions to the principal propagation characteristics—the phase change, the birefringence, and the attenuation coefficient—as a function of voltage across the waveguide.

Manuscript received June 13, 1991; revised September 18, 1991. This work was supported by the Department of Energy.

The authors are with the Department of Electrical Engineering, University of Maryland, Baltimore, MD 21228.

IEEE Log Number 9104261.

Description of the Method

A finite element method has been used to determine the propagation constant and mode field distribution of the ridge

waveguide for both TE and TM polarizations in the absence of the QW. The effective index method yields an approximate propagation constant, but the accuracy is limited. Also, the mode field distribution cannot be accurately obtained. The scalar finite element method [2] has been chosen since it is far simpler to implement, less troubled by spurious modes, and is computationally less intensive than the full vector finite element method, while yielding propagation constants which are nearly identical except near cutoff. The scalar approximation for the HE mode is found by minimizing the functional

$$L = \int\int \left[\left(\frac{\partial \phi}{\partial x} \right)^2 + \left(\frac{\partial \phi}{\partial y} \right)^2 - k_0^2 n^2 \phi^2 + \beta^2 \phi^2 \right] dS \quad (1)$$

and the scalar approximation for the EH mode is found by minimizing the functional

$$L = \int\int \left[\left(\frac{1}{n} \frac{\partial \phi}{\partial x} \right)^2 + \left(\frac{1}{n} \frac{\partial \phi}{\partial y} \right)^2 + \frac{\beta^2}{n^2} \phi^2 - k_0^2 \phi^2 \right] dS \quad (2)$$

where ϕ is the scalar field, n is the index of refraction, x and y are the coordinates transverse to the mode propagation, k_0 is the vacuum wavenumber, and β is the propagation constant for which we are solving. Discretization of (1) and (2) yields the finite element equations [2].

A finite element code has also been used to evaluate the electrostatic field distribution. It calculates the electric field inside the waveguide, given the imposed voltage, from which the parallel and perpendicular electrostatic fields at the quantum well can be computed. The electric field dependent parameters of the quantum well can then be evaluated.

Quantum well devices use the presence of strong excitonic resonances at the band edge. These resonances shift to longer wavelengths while remaining resolved as the electrostatic field increases perpendicular to the QW layer. This shift has been called the quantum confined stark effect. It was first seen and explained by Miller *et al.* [3] and subsequently modeled by others [4], [5]. The dielectric function of the GaAs QW layer [6] at a photon energy ω, near the 2-D band edge is

$$\epsilon_{QW}(\omega) = \epsilon_G(\omega) + 4\pi\beta_H \omega_H^2 / (\omega_H^2 - \omega^2 - i\omega\Gamma_H) + 4\pi\beta_L \omega_L^2 / (\omega_L^2 - \omega^2 - i\omega\Gamma_L) \quad (3)$$

where the first term, $\epsilon_G(\omega)$, is the background dielectric function of the GaAs QW layer in the absence of excitons, and the other two terms are the heavy-hole and light-hole excitonic dielectric functions given in terms of the Lorentzian oscillator model. The quantities ω_x and Γ_x are the excitonic energy and linewidth and β_x is the oscillator strength of the exciton where $x = H$ or L refers respectively to the heavy and light holes.

The excitonic energy ω_x and hence the peak absorption is assumed to vary quadratically with an increasing perpendicular electrostatic field across the QW in accordance with experimental results [6]. The change in the parameters due to parallel electrostatic fields arising from the geometry of the waveguide were also considered along with the perpendicular fields to evaluate the quantum well effects. The effects of the parallel fields are linearly extrapolated from the experimental results of Miller *et al.* [3] over the entire range of electric field strengths.

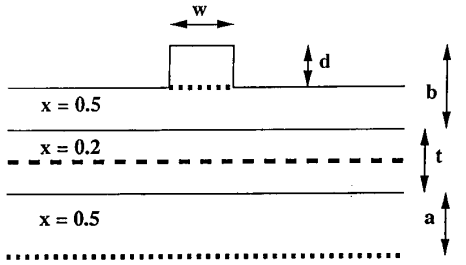

Fig. 1. Cross section of the GaAs/AlGaAs ridge waveguide structure. The dashed line shows the position of the quantum well which is 100 Å. The dimensions chosen are $w = 3.0$ μm, $d = 1.1$ μm, $b = 1.4$ μm, $t = 0.2$ μm, and $a = 0.3$ μm. The Al concentration in different layers of $Al_xGa_{1-x}As$ layers is shown. The regions of applied voltage are shown as dotted lines.

The change in the propagation constant of the ridge waveguide due to the electric field induced changes in the refractive index of the thin QW layer has been calculated perturbatively using the following equation [7]:

$$\delta\beta^2 = k_0^2 \frac{\int \phi^* \delta n^2 \phi \, dS}{\int |\phi|^2 \, dS}. \quad (4)$$

Results

The ridge waveguide geometry which we studied is shown in Fig. 1. The depth of the ridge is chosen to give single mode operation and good confinement of the mode in the ridge region. We assume that the ridge is highly conducting so that the voltage from a metallized strip on top of the ridge is applied at the bottom. The structure is assumed to be grounded below the $x = 0.5$ layer at a depth of 0.8 μm by a highly conducting substrate. The effects due to free carrier absorption is not included in the calculations. The following parameters are assumed when (3) is used: $4\pi\beta_H^{TE} = 0.00465$, $4\pi\beta_L^{TE} = 0.00151$, $4\pi\beta_H^{TM} = 0$, $4\pi\beta_L^{TM} = 0.00565$, $\Gamma_H = 8.4$ meV, and $\Gamma_L = 10.0$ meV. The quantities ω_H and ω_L have been determined from the width of the quantum well and the Al concentration of the surrounding material.

Fig. 2 compares the absorption and the phase coefficients obtained with the full mode analysis as outlined in the previous section and a simple slab analysis. The comparison in Fig. 2 is shown for 0.87 μm wavelength and TE polarization. The same comparison is shown in Fig. 3 for TM polarization. Results that do not include the parallel electrostatic fields in the calculations are also shown. As can be seen from the figures, the parallel field contribution is not significant in this case, the reason being that the parallel fields generated are small and are localized to small areas of the QW. There is a slight reduction in the peak absorption, which is consistent with previous results in slab waveguides [3].

Figs. 4 and 5 depict the calculated absorption and phase

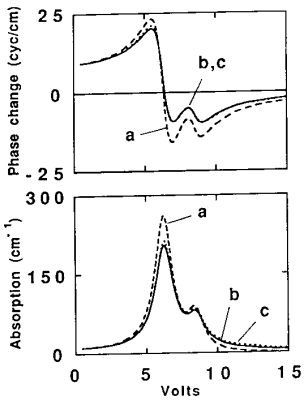

Fig. 2. Absorption coefficient and phase change versus applied voltage for the fundamental TE mode at 0.87 μm wavelength. (a) (dashed line) Results obtained from a simple slab model. (b) (solid line) Results obtained retaining the full geometry. (c) (dotted line) Results obtained without considering the effect of the parallel electrostatic field. The solid and dotted lines are nearly coincident, indicating that the parallel electrostatic field has little effect.

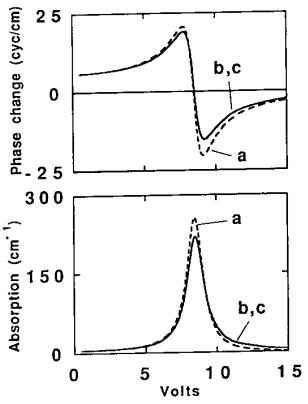

Fig. 3. Absorption coefficient and phase change versus applied voltage for the fundamental TM mode at 0.87 μm wavelength. (a)-(c) are the same as in Fig. 2.

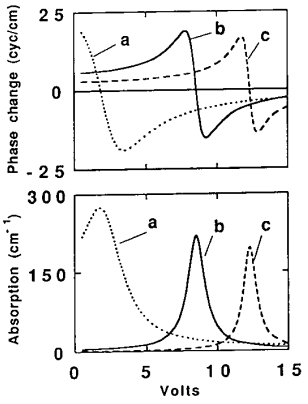

Fig. 5. Absorption coefficient and phase change versus applied voltage for the fundamental TM mode at wavelengths of (a) 0.85 μm, (b) 0.87 μm, and (c) 0.89 μm.

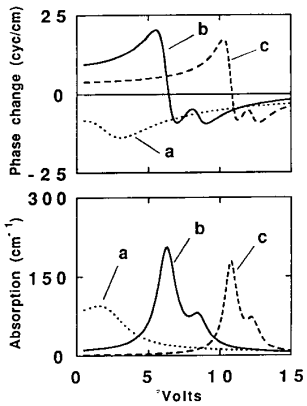

Fig. 4. Absorption coefficient and phase change versus applied voltage for the fundamental TE mode at wavelengths of (a) 0.85 μm, (b) 0.87 μm, and (c) 0.89 μm.

changes for TE and TM polarizations at 0.85, 0.87, and 0.89 μm wavelengths. The optimal wavelength to use in an interferometric switch or any device which utilizes the phase change due to the QW would be 0.89 μm as the voltage required to alter the phase by a factor of two would not introduce much attenuation.

Conclusions

In this letter, we have presented a method for calculating the propagation characteristics of a ridge waveguide with a QW layer. The approach we use allows us to disentangle geometric effects from the physical effects due to the excitonic resonances in QW. We find that a simple slab approach overestimates the attenuation and phase change for wavelengths smaller than the peak absorption wavelength and underestimates them for wavelengths larger than the peak absorption wavelength of the QW. The approach we are using shows great promise for determining the propagation

characteristics in a wide variety of "band-gap engineered" devices.

ACKNOWLEDGMENTS

We gratefully acknowledge useful discussions with Dr. A. T. Drobot and Dr. A. Friedman. Computational work was carried out at the San Diego Supercomputer Center and the National Energy Research Supercomputing Center.

REFERENCES

[1] T. H. Wood, "Direct measurement of the electric-field- dependent absorption coefficient in GaAs/AlGaAs multiple quantum wells," *Appl. Phys. Lett.*, vol. 48, pp. 1413-1415, 1986.

[2] N. Mabaya, P. E. Lagasse, and P. Vandenbulcke, "Finite element analysis of optical waveguides," *IEEE Trans. Microwave Theory Tech.*, vol. MTT-29, pp. 600-605, 1981.

[3] D. A. B. Miller, D. S. Chemla, T. C. Damen, A. C. Gossard, W. Wiegmann, T. H. Wood, and C. A. Burrs, "Electric field dependence of optical absorption near the band gap of quantum-well structures," *Phys. Rev.*, vol. 32, pp. 1043-1060, 1985.

[4] K. B. Kahen, and J. P. Leburton, "Exciton effects in the index of refraction of multiple quantum wells and superlattices," *Appl. Phys. Lett.*, vol. 49, pp. 734-736, 1986.

[5] G. J. Sonek, J. M. Ballantyne, Y. J. Chen, G. M. Carter, S. W. Brown, E. S. Koteles, and J. P. Salerno, "Dielectric properties of GaAs/AlGaAs multiple quantum well waveguides," *IEEE J. Quantum Electron.*, vol. QE-22, pp. 1015-1018, 1986.

[6] Y. J. Chen, C. Jagannath, G. M. Carter, E. S. Koteles, and S. W. Brown, "Optical properties of GaAs/AlGaAs multiple quantum well waveguides," *Superlattices and Microstructures*, vol. 3, pp. 287-290, 1987.

[7] P. Yeh, *Optical Waves in Layered Media*. New York: Wiley, 1988, pp. 351-374.

Alignable Epitaxial Liftoff of GaAs Materials with Selective Deposition Using Polyimide Diaphragms

C. Camperi-Ginestet, M. Hargis, N. Jokerst, and M. Allen

Abstract—**In this letter we report the selective and alignable deposition of patterned thin-film epitaxial GaAs/GaAlAs devices onto a host substrate such as silicon for low cost, manufacturable hybrid integrated optoelectronic circuits. We use a thin polyimide diaphragm as the transparent transfer medium for these patterned epitaxial devices. Each of these devices or a group of these devices on the polyimide is then optically aligned and selectively deposited onto the host substrate. Using this technique, a light emitting diode 50 × 50 μm in area and 2 μm thick was grown on a GaAs substrate, lifted off, aligned and selectively deposited onto a silicon host substrate, and electrically contacted and tested. Using this method, the sparse distribution of costly photonic devices or the deposition of aligned arrays of devices to fabricate larger arrays without large area growth of photonic devices can be achieved on a variety of smooth host substrates.**

INTRODUCTION

THE monolithic integration of gallium arsenide (GaAs) photonic and electronic materials and devices with host substrates, such as silicon (Si), glass, and polymers, will enable the fabrication of the next generation of optoelectronic integrated circuits (OEIC's). These OEIC's are currently costly and complicated to fabricate in comparison to silicon integrated circuits. If conventional microelectronic processing techniques could be used in the fabrication of such OEIC's, their cost would be reduced and their manufacture would become more attractive to industry. In this letter, we discuss an improved method for the alignment, selective deposition, and interconnection of thin-film epitaxial GaAs devices onto host substrates such as Si.

A standard technique for GaAs on Si integration is heteroepitaxial growth [1]. However, the crystal quality of this material is often insufficient for many optical applications. One integration method which seeks to preserve the high material quality of lattice-matched growth is the epitaxial liftoff (ELO) process as described by Bellcore [2]. A thin aluminum arsenide (AlAs) sacrificial layer is grown on a GaAs substrate, and GaAs device epilayers are grown on top of this AlAs layer. The GaAs lattice matched epilayers are separated from the growth substrate by selectively etching the AlAs sacrificial layer. These device layers are then mounted in a hybrid fashion onto a variety of substrates. This ELO material is very high quality [2] and is currently being used for the integration of GaAs materials onto host substrates such as Si, glass, lithium niobate, and polymers [2]–[5].

Although the Bellcore technique yields high quality material, it has several problems, including the inability to align

Manuscript received July 22, 1991; revised September 9, 1991. This work was supported by the Newport Corporation, Digital Equipment Corporation, and the National Science Foundation under the Presidential Young Investigator Program (NJ). Microfabrication was carried out in the Microelectronics Research Center (MiRC) of Georgia Tech with fabrication assistance from the MiRC staff.

The authors are with the School of Electrical Engineering, Microelectronics Research Center, Georgia Institute of Technology, Atlanta, GA 30332.

IEEE Log Number 9104470.